Notch1/Hes1-PTEN/AKT/IL-17A feedback loop regulates Th17 cell differentiation in mouse psoriasis-like skin inflammation

YA-WEN LIN[1*], XIN-XIN LI[1,2*], FANG-HUI FU[1], BIN LIU[3], XIAOYUN XING[1], RUIQUN QI[4] and LEI MA[1]

[1]Department of Dermatology, Binzhou Medical University Hospital, Binzhou, Shandong 256603;
[2]Department of Dermatology, Liaocheng Veterans Hospital, Liaocheng, Shandong 252000;
[3]Institute for Metabolic and Neuropsychiatric Disorders, Binzhou Medical University Hospital,
Binzhou, Shandong 256603; [4]Department of Dermatology, The First Affiliated Hospital of
China Medical University, Shenyang, Liaoning 110001, P.R. China

Abstract. IL-17A, the effector cytokine of T helper (Th) 17 cells, plays a crucial role in the pathogenesis of psoriasis. The Notch1 and PI3K/AKT signaling pathways are implicated in Th17 cell differentiation and IL-17A production. The present study aimed to evaluate the regulatory effect of the Notch1/hairy and enhancer of split 1 (Hes1)-PTEN/AKT/IL-17A feedback loop on Th17 cell differentiation via the PI3K/AKT inhibitor LY294002 in a mouse model of psoriasis. Mice were randomly divided into 3 groups: a control group, a model group [5% imiquimod (IMQ)-induced group] and an intervention group (5% IMQ-induced plus LY294002-treated group). Skin structural characteristics were recorded and evaluated by hematoxylin and eosin staining. The weights of the spleens and inguinal lymph nodes were measured. Th17 cell percentage, as well as the mRNA and protein expression levels of Notch1, Notch1 intracellular domain (NICD1), Hes1, PTEN, AKT, phosphorylated (p)-AKT, mTOR complex 1 (mTORC1), p-mTORC1, S6 kinase (S6K)1, S6K2 and IL-17A were detected in skin samples of the three experimental groups. Additionally, splenic mononuclear cells from model mice were treated by 10 and 50 μM LY294002 to further evaluate its regulatory effect on Notch1/Hes1-PTEN/AKT/IL-17A feedback loop. Increased Th17 cell percentage, increased expression of Notch1, NICD1, Hes1, AKT, p-AKT, mTORC1, p-mTORC1, S6K1, S6K2 and IL-17A, and decreased PTEN levels were observed in model mice alongside marked psoriasis-like skin inflammation, splenomegaly and lymphadenopathy. LY294002 treatment significantly alleviated the severity of psoriasis-like skin inflammation in the intervention mice, attenuated the degree of epidermal hyperplasia and dermal inflammatory cell infiltration, and mitigated splenomegaly and lymphadenopathy. In addition, LY294002 treatment reversed the increased Th17 cell percentage, as well as the increased expression of Notch1, NICD1, Hes1, AKT, p-AKT, mTORC1, p-mTORC1, S6K1, S6K2 and IL-17A, and the decreased expression of PTEN. *In vitro* study from 5% IMQ-induced mouse splenic mononuclear cells presented that high dose of LY294002 exerted more obviously regulatory effect on Notch1/Hes1-PTEN/AKT/IL-17A feedback loop. The current findings suggested that the Notch1/Hes1-PTEN/AKT/IL-17A feedback loop regulates Th17 cell differentiation within the disease environment of psoriasis. Blocking the Notch1/Hes1-PTEN/AKT/IL-17A feedback loop may thus be a potential therapeutic method for management of psoriatic inflammation.

Introduction

Psoriasis is an immune-mediated chronic inflammatory skin disease, in which intralesional T lymphocytes and their proinflammatory signals trigger keratinocytes to rapidly proliferate and initiate the inflammatory process (1). Previous studies reported that the IL-23/T helper (Th)17 axis played a crucial role in the pathogenesis of psoriasis (2,3). IL-17A is the most important effector cytokine of Th17 cells, which is overexpressed in psoriasis, resulting in apparent epidermal hyperplasia and inflammatory reaction. Targeted anti-IL-17 therapies have been demonstrated to be of great efficacy in moderate and severe plaque psoriasis (4). Furthermore, in a mouse model of psoriasis, the crucial roles of IL-17 have also been demonstrated (5).

Notch signaling is an evolutionarily conserved intracellular signal transduction system, which is involved in the regulation of processes of differentiation, proliferation, migration and apoptosis of epidermal cells, and participates in the pathogenesis of certain human skin diseases, including psoriasis (6). In mammals, four Notch receptors (Notch1, 2, 3 and 4) and five

Correspondence to: Dr Lei Ma, Department of Dermatology, Binzhou Medical University Hospital, 661 Second Huanghe Road, Binzhou, Shandong 256603, P.R. China
E-mail: doctor_malei@hotmail.com

*Contributed equally

ligands (jagged 1 and 2, as well as δ-like 1, 3 and 4) have been confirmed. Although the process of activation and transduction of Notch signaling is complex, in essence, it involves the cleavage of cytoplasmic Notch by γ-secretase and the release of the Notch intracellular domain (NICD) that possesses a nuclear localization signal (NLS) that can translocate signals to the nuclei and further regulate downstream target genes, such as hairy and enhancer of split 1 (Hes1) (7). Notch signaling has been reported to be crucial for Th17 cell differentiation, which is activated in Th17 cell polarized conditions in humans and mice (8-12). A previous study suggested that blocking Notch signaling with a γ-secretase inhibitor could significantly alleviate mouse psoriasis-like skin inflammation, which resulted in a dose-dependent decrease in the percentage of Th17 cells and its transcription factor RAR-related orphan receptor (RORγt), as well as a decrease in Notch1, Hes1 and IL-17A mRNA expression and IL-17A secretion in splenic CD4+ T cells in a 5% imiquimod (IMQ)-induced mouse psoriasis-like skin model, indicating that Notch1/Hes1 signaling can regulate Th17 cell differentiation and function in the disease-specific inflammation of psoriasis (13). NF-KB activator1(Act1) is an important adaptor molecule in IL-17 signaling transduction (14), which can interact with Notch1 signaling and form an Act1-NICD1 complex to induce Notch1 activation and facilitate IL-17 crosstalk with Notch1 signaling (15).

PI3K/AKT (also called protein kinase B) and mTOR signaling is important in the regulation of innate and adaptive immune responses (16), which has been reported to be upregulated in lesions of patients with psoriasis and in IMQ-induced mouse psoriasiform inflammation (17,18). mTOR exists in two distinct protein complexes, namely mTORC1 and mTORC2. PI3K/AKT/mTORC1 signaling has been reported to positively regulate Th17 cell differentiation through several means, including the regulation of transcription factor hypoxia-inducible factor 1α expression, signal transducers and activators of transcription 3 tyrosine phosphorylation, downregulation of the Th17 cell differentiation negative regulator growth factor independent 1 (Gfi1) and RORγt nuclear translocation (19,20), among which, Gfi1 expression and RORγt nuclear translocation are dependent on the signaling molecules 40S ribosomal S6 kinase (S6K)1 and S6K2, which are located downstream of mTORC1. Gfi1 expression is suppressed by the transcription factor early growth response protein 2, which is positively regulated by S6K1 (19). RORγt does not possess a NLS but is localized in the nuclei of Th17 cells. S6K2, the nuclear counterpart of S6K1, possesses a RORγt-associated NLS, and can bind and transport RORγt to nuclei. Thus, mTORC1 can accelerate RORγt translocation into nuclei during Th17 differentiation (19). PTEN is the critical negative regulator of PI3K/AKT/mTOR signaling, which was reported to be a target of activated Notch1 in T-cell acute lymphoblastic leukemia, via Hes1-mediated suppression of the PTEN promoter (21,22). In addition, the regulatory function of the Notch1/Hes1/PTEN axis has also been identified in other human diseases, including asthma, diabetic nephropathy and hepatocellular carcinoma (23-27). Based on these previous studies and our previous research, it could be hypothesized that a feedback loop between Notch1 and IL-17A exists via the Notch1/Hes1-PTEN/AKT/mTORC1 signaling axis within the pathological environment of psoriasis. Thus,

PI3K/AKT signaling was blocked in the present study using LY294002 to explore the possible regulatory effect of the Notch1/Hes1-PTEN/AKT/IL-17A feedback loop on Th17 cell differentiation and IL-17A production in mouse psoriasis-like skin inflammation.

Materials and methods

Mice and treatment. A total of 24 male BALB/c mice (age, 6-8 weeks old; weight range, 16-20 g) were purchased from Jinan Pengyue Experimental Animal Breeding Co., Ltd., China and bred in a specific pathogen-free environment in the animal center of Binzhou Medical University Hospital (Binzhou, China). They were group-housed at up to five mice per cage in a ventilated, temperature-controlled 23±1℃, 55% relative humidity condition with a 12-h light/dark cycle. Autoclaved water and food were available *ad libitum* to mice. The experimental mice were randomly divided into 3 groups, namely the control group (n=8), the model group (5% IMQ-induced group; n=8) and the intervention group (5% IMQ-induced plus LY294002-treated group; n=8). Daily topical application of 5% IMQ cream (62.5 mg; 3M Health Care Limited) on the shaved back skin of the model and intervention mice were employed to induce psoriasis-like skin inflammation in these groups, as previously described (5), while an equivalent quantity of Vaseline (Qingdao Hainuo Biological Engineering Co., Ltd.) was applied to the control mice. LY294002 (cat. no. HY-10108; MedChemExpress) dissolved in DMSO (cat. no. D2650; Sigma-Aldrich; Merck KGaA) was intraperitoneally injected (10 mg/kg/day) in the intervention mice since the beginning of IMQ application. Control and model mice received an equivalent volume of DMSO intraperitoneal injection. The experimental mice were anesthetized by 4% isoflurane for the induction and 2% for the maintenance to complete daily treatment. After 6 consecutive days, mice were euthanized by inhaling 10% isoflurane for 5 min. Animal death was confirmed by observing respiratory and cardiac arrest and the absence of active paw reflex for >5 min. Next, the skin tissues, inguinal lymph nodes and spleens were acquired to conduct subsequent experiments. During the experimental process, if their weights reduced 20%, the skins occurred infection and suppuration or they appeared obvious fidgety, mice would be subjected to euthanasia. All animal procedures were approved (approval no. 20190104-15) by the Laboratory Animal Ethics Committee of Binzhou Medical University Hospital (Binzhou, China), followed the 3R-principle (replacement, reduction, refinement) and carried out in accordance with the UK Animals (Scientific Procedures) Act, 1986, and associated guidelines, and the EU Directive 2010/63/EU for animal experiments.

Skin structural characteristics scoring and histopathological examination. Changes in skin structural characteristics were recorded daily, and the severity of psoriasis-like inflammation was estimated by the target lesion score based on the clinical psoriasis area and severity index (5). Erythema, thickening and scaling were scored on a scale from 0 to 4. The cumulative score of the three indicators from 0 to 12 served as a measure of the severity of psoriasis-like inflammation. Skin samples

were fixed in 10% neutral formalin for 24 h at 4°C, embedded with paraffin, sectioned, and stained with hematoxylin and eosin using standard procedures (hematoxylin staining for 8 min and eosin staining for 1 min at room temperature) (28). Histopathological characteristics were evaluated by well-trained pathologists in a double-blinded manner. Image-Pro Plus 6.0 imaging system (Media Cybernetics, Inc.) was employed to measure the epidermis thickness from the stratum corneum to the basement membrane.

Preparation of single cell suspension from skin tissues and spleen. Skin samples were cut into 0.5 cm x 0.5 cm pieces and incubated in the presence of 0.5% trypsin (cat. no. Y0002311; Sigma-Aldrich; Merck KGaA) at 37°C for 2 h. Upon separation of the epidermis, the dermis was digested with DNase I (cat. no. D8071; Beijing Solarbio Science & Technology Co., Ltd.) and collagenase IV (cat. no. C5138; Sigma-Aldrich; Merck KGaA) in DMEM (cat. no. E600008-0500; Sangon Biotech Co., Ltd.) for 37°C, 1 h. Cells were harvested and resuspended ($1x10^6$ cells/ml) for use in subsequent flow cytometry analysis.

Spleen samples were triturated and filtered through cell strainers (70 and 40 μm; cat. no. F613462 and F613461; Sangon Biotech Co., Ltd.). Cell suspension was collected and treated according to the protocol of mouse splenic mononuclear cell isolation kit (cat. no. LDS1090PK; Tianjin Haoyang Biological Products Technology Co., Ltd.). Splenic mononuclear cells were acquired and suspended in RPMI-1640 medium (cat. no. E600028; Sangon Biotech Co., Ltd.) with 10% fetal bovine serum (cat. no. E510008-0500; Sangon Biotech Co., Ltd.), 1% penicillin-streptomycin liquid, 1% nonessential amino acid and 0.01% β-mercaptoethanol (cat. nos. P1400, N1250 and M8210, respectively; Beijing Solarbio Science & Technology Co., Ltd.). Then cells were counted and adjusted to 10^6 cells/ml for subsequent treatment and experiments.

Splenic mononuclear cells treatment by LY294002. Splenic mononuclear cells isolated from 5% IMQ-induced model mice were divided into 0, 10 and 50 μM LY294002-treated group. In LY294002-treated groups, LY294002 was dissolved in DMSO. At the same time, splenic mononuclear cells isolated from control mice were used as control group and treated with DMSO only.

Flow cytometric analysis of the proportion of Th17 cells (IL-17A$^+$ CD4$^+$ T cells/CD4$^+$ T cells). Cells were firstly stimulated with phorbol 12-myristate 13-acetate, ionomycin, brefeldin A and monensin (Cell Stimulation Cocktail Plus Protein Transport Inhibitors; cat. no. 4975; eBioscience; Thermo Fisher Scientific, Inc.) for 4 h at 37°C under 5% CO_2. Next, the cells were collected (630 x g for 10 min at room temperature), washed two times with ice-cold phosphate-buffered saline (PBS) (cat. no. E607008-0500; Sangon Biotech Co., Ltd.) and surface-stained with an Allophycocyanin (APC) anti-mouse CD4 Antibody (0.8 μg/ml, cat. no. 100516; BioLegend, Inc.) for 30 min at 4°C in the dark. Next, the cells were fixed and permeabilized using Perm/Fix (cat. no. 88-8824-00; eBioscience) solution and intracellularly stained with a P-phycoerythrin (PE) anti-mouse IL-17A Antibody (2.5 μg/ml, cat. no. 506904; BioLegend, Inc.) for

30 min at 4°C in the dark. Detection and analysis were conducted with a FACSCanto flow cytometer (BD Biosciences). The characterized phenotype of Th17 cells was IL-17A$^+$ CD4$^+$ and the results are expressed as a percentage of total CD4$^+$ T cells.

Reverse transcription-quantitative PCR (RT-qPCR) analysis. According to the manufacturer's instructions, total RNA was extracted from each skin sample and spleen using TRIzol® (cat. no. B511311; Sangon Biotech Co., Ltd.). The purity and integrity of each RNA sample were confirmed, respectively, by measuring an absorbance 260/A280 ratio of 1.8-2.0, as detected by spectrophotometry (NV3000; Vastech Inc.), and by observing intact 28S and 18S ribosomal RNA bands with a 2:1 ratio in 1.5% agarose gel electrophoresis with AG-CelRed Nucleic acid gel stain (cat. no. AG11918; Hunan Accurate Biotechnology Co., Ltd.). cDNA was synthesized utilizing the Evo M-MLV Mix Kit with gDNA Clean for qPCR (cat. no. AG11728; Hunan Accurate Biotechnology Co., Ltd.) according to the manufacturer's protocols. RT-qPCR was performed with gene-specific primers using SYBR® Green Premix Pro Taq HS qPCR kit (cat. no. AG11701; Hunan Accurate Biotechnology Co., Ltd.) on a CFX96 Touch™ Real-Time PCR Detection System (Bio-Rad Laboratories, Inc.). All primers were designed by Hunan Accurate Biotechnology Co., Ltd. The National Center for Biotechnology Information accession numbers are as follows: 14433 (GAPDH), 18128 (Notch1), 15205 (Hes1), 19211 (PTEN), 11651 (AKT), 74370 (mTORC1), 72508 (S6K1), 58988 (S6K2) and 16171 (IL-17A). The primer sequences were as follows: Notch1 sense, 5'-TGCCAGTATGATGTG GATGAG-3' and antisense, 5'-GGTCCCTGTGTAACCTTC TGT-3'; Hes1 sense, 5'-AGCCCACCTCTCTCTTCTGA-3', and antisense, 5'-AGGCGCAATCCAATATGAAC-3'; PTEN sense, 5'-AAGGGACGGACTGGTGTAATGATTTG-3' and antisense, 5'-CGCCTCTGACTGGGAATTGTGAC-3'; AKT sense, 5'-GACTGACACCAGGTATTTCGATGA-3' and antisense, 5'-CTCCGCTCACTGTCCACACA-3'; mTORC1 sense, 5'-CCATCGGTGCAAACCTACAG-3' and antisense, 5'-TCCATTCACTGTAGGCCTGG-3'; S6K1 sense, 5'-TTC TGTCGGGAGTAGCACTG-3' and antisense, 5'-CCCCTT TACCAAGTACCCGA-3'; S6K2 sense, 5'-TCACTGCAG AGAACCGGAAGA-3' and antisense, 5'-GGGGTTCCGCTT CAGAAACTT-3'; IL-17A sense, 5'-TTTAACTCCCTTGGC GCAAAA-3' and antisense, 5'-CTTTCCCTCCGCATTGAC AC-3'; and GAPDH sense, 5'-AAATGGTGAAGGTCGGTG TGAAC-3' and antisense, 5'-CAACAATCTCCACTTTGC CACTG-3'. The thermocycling conditions were as follows: 95°C for 5 min, followed by 40 cycles of denaturation for 10 sec at 95°C and annealing/elongation for 30 sec at 60°C. GAPDH was used as the internal control, and the expression levels of target genes were calculated based on the following formula $2^{-\Delta\Delta Cq}$ ($\Delta\Delta Cq=\Delta Cq$-treated-$\Delta Cq$-control) (29).

Western blot detection and analysis. Total protein from skin samples and treated splenic mononuclear cells were extracted using RIPA lysis buffer (cat. no. R0020; Beijing Solarbio Science & Technology Co., Ltd.). Equal quantities of denatured protein (50 μg) were separated by 10% sodium dodecyl sulphate-polyacrylamide gel electrophoresis and transferred to polyvinylidene fluoride (cat. no. ipvh00010; Sigma-Aldrich;
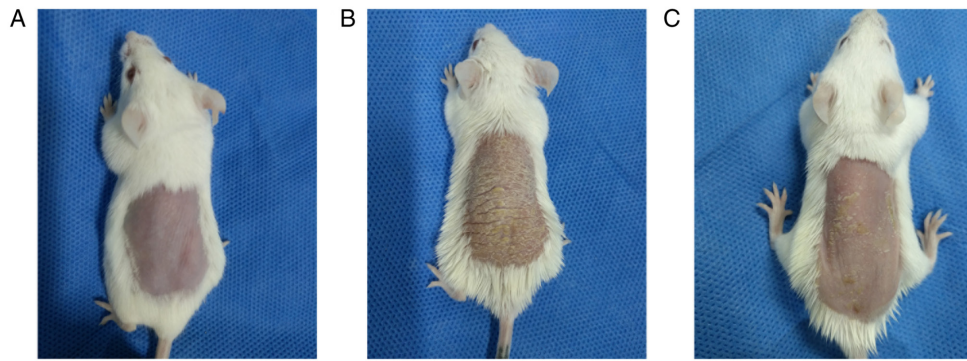
Figure 1. Structural characteristics of the skin of the experimental mice. (A) Control mice did not present any signs of erythema, scaling or thickening. (B) Model mice displayed significant signs of psoriasis-like inflammation. (C) Intervention mice showed similar signs of psoriasis-like inflammation as model mice; however, the degree of severity was notably alleviated compared with model mice.

Merck KGaA) membranes. After blocking in 5% skim milk in 0.1% TBS-Tween 20 (TBST; cat. no. T1082; Beijing Solarbio Science & Technology Co., Ltd.) for 2 h at room temperature, the membranes were incubated overnight at 4°C with primary antibodies (all from Affinity Biosciences) against Notch1 (1:1,000; cat. no. AF5307), NICD1 (1:1,000; cat. no. AF5307), Hes1 (1:1,000; cat. no. AF7575), PTEN (1:1,000; cat. no. AF6351), AKT (1:1,000; cat. no. AF6261), phosphorylated (p)-AKT (Thr308) (1:1,000; cat. no. AF3262), p-AKT (Ser473) (1:1,000; cat. no. AF0016), mTORC1 (1:1,000; cat. no. AF6308), p-mTOR (Ser2448) (1:1,000, cat. no. AF3308), S6K1 (p70S6K) (1:1,000; cat. no. AF6226), S6K2 (p70S6kβ) (1:1,000; cat. no. AF3486) and IL-17A (1:1,000; cat. no. DF6127). The next day, each membrane was washed 3 times for 5 min with 0.1%TBST, on a shaking table, at room temperature. The membranes were incubated with the corresponding horseradish peroxidase-conjugated goat anti-rabbit IgG antibodies (1:1,000; cat. no. 14708; Cell Signaling Technology, Inc.) for 1 h at room temperature. Anti-GAPDH antibody (1:1,000; cat. no. AF7021; Affinity Biosciences) was used to confirm equal protein loading in each lane. The protein bands were detected using ECL kit (cat. no. MA0186; Dalian Meilun Biology Technology Co., Ltd.) and x-ray film, and were quantified using ImageJ software v 4.1 (National Institutes of Health).

Statistical analysis. Shapiro-Wilk test was performed to evaluate the normality of the data, and the data were expressed as the means ± SD or median (interquartile range). According to Levene's test of homogeneity of variance, one-way ANOVA was used to compare the differences among the experimental groups for homogeneous variance, followed by Student-Newman-Keuls (SNK) or Tukey's test performing the multiple comparison for three groups or four groups respectively; Welch ANOVA followed by Tamhane's T2 test was used for comparison of heterogeneous variance. Kruskal-Wallis H test followed by the Dunn-Bonferroni test were used to analyze the abnormally distributed data. The difference of lesions' scores was analyzed with the method of repeated measures ANOVA followed by Bonferroni's adjustments. Data were analyzed using SPSS 19.0 (IBM Corp.) and GraphPad Prism 5 (GraphPad Software, Inc.). $P < 0.05$ was considered to indicate a statistically significant difference.

Results

LY294002 alleviates the severity of psoriasiform skin lesions. Control mice presented no signs of erythema, thickening or scaling during the 6 days. By contrast, the model mice presented signs of psoriasis-like inflammation on their shaved back skin from the second day onwards, which exacerbated progressively and was most severe on the 6th day. LY294002 inhibition alleviated the degree of erythema, thickening and scaling in the intervention mice (Fig. 1). The scores of lesions of control mice, model mice and intervention mice were listed in Table I and were significantly different among the three experimental groups ($F = 1751.182$, $P < 0.01$); moreover, the differences between every two experimental groups were significant (all $P < 0.01$).

LY294002 attenuates the pathological characteristics of psoriasiform skin lesions. Histopathological examination revealed that, in control mice, the epidermis was thin and consisted of 1-2 cell thick layers. Model mice presented marked epidermal hyperplasia with hyperkeratosis, trochanterellus extension, parakeratosis with Munro's micro-abscess, extensive inflammatory cell infiltration and dermal telangiectasias, which were similar to previously reported findings and matched the pathological characteristics of psoriasis (5). Compared with the model group, LY294002 inhibition notably ameliorated the degree of epidermal hyperplasia and dermal inflammatory cell infiltration in the intervention group (Fig. 2). Further comparison of epidermal thickness showed significant differences among the three groups ($F = 192.233$; $P < 0.01$) and between two groups (model mice, 104.669 ± 11.127 μm vs. intervention mice, 49.983 ± 7.656 μm and control mice, 26.480 ± 4.301 μm; all $P < 0.01$).

LY294002 mitigates splenomegaly and lymphadenopathy. The volumes of the spleen and inguinal lymph nodes in model mice were significantly larger than those of the spleen and inguinal lymph nodes of control mice, while lessened after intervention with LY294002 (Fig. 3). As shown in Table II, compared with those of control mice, the spleen weight and index of model mice were significantly increased (both $P < 0.01$). However, upon AKT inhibition by LY294002, they were markedly decreased in the intervention mice (both $P < 0.01$). In parallel with the changes in spleen, the weight of inguinal lymph nodes notably increased in the model mice compared with that of the

Table I. Psoriasis area and severity index scores of experimental mice.

Group	Day 1	Day 2	Day 3	Day 4	Day 5	Day 6
Control mice	0.000±0.000	0.000±0.000	0.000±0.000	0.000±0.000	0.000±0.000	0.000±0.000
Model mice	0.000±0.000	2.875±0.354	5.500±0.535	7.00±0.535	8.625±0.518	10.125±0.835
Intervention mice	0.000±0.000	2.000±0.535[a]	3.625±0.518[a]	4.375±0.518[a]	6.500±0.535[a]	6.000±0.535[a]

Data are presented as the means ± SD. Repeated measures ANOVA followed by Bonferroni's adjustments are used for statistical analysis. [a]$P<0.01$ vs. Model.
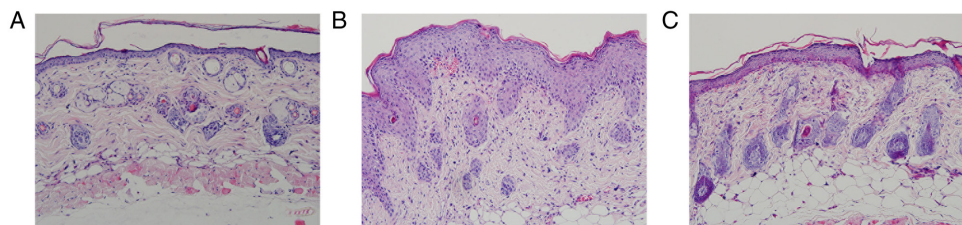

Figure 2. Pathological characteristics of experimental mice (hematoxylin and eosin staining; magnification, x200). (A) Control mice presented a thin epidermis layer, which was composed by only 1-2-layer epidermal cells. (B) Model mice presented notable epidermal hyperplasia with hyperkeratosis, trochanterellus extension, parakeratosis with Munro's micro-abscess, extensive inflammatory cell infiltration and dermal telangiectasias. (C) Intervention mice exhibited markedly reduced epidermal hyperplasia and dermal inflammatory cell infiltration.
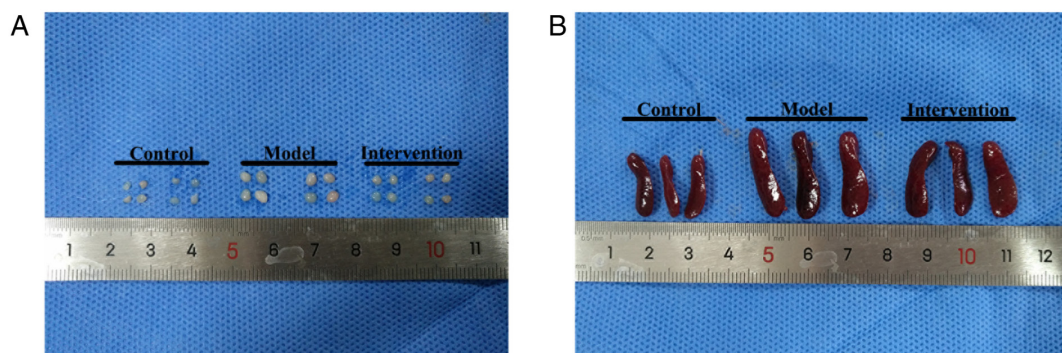

Figure 3. Comparison of the size of (A) inguinal lymph nodes and (B) spleen among the experimental mice.

control mice, and upon LY294002 treatment, it was markedly reduced in the intervention mice (both $P<0.01$; Table II).

LY294002 inhibition reduces Th17 cell percentage. Representative images of Th17 cell percentage and IL-17A+ CD4+ cells gated on CD4+ T cells in the three aforementioned groups are shown in Fig. 4. There were significant differences in Th17 cell percentage in the skin tissues among the three experimental groups (F=8.482; $P<0.01$), which was markedly higher in model mice (20.521±8.023%) than in the control mice (6.670±3.545%; $P<0.01$). However, upon LY294002 treatment, the Th17 cell percentage significantly decreased in the intervention mice (11.540±5.278%) compared with that in the model mice ($P<0.05$).

LY294002 inhibition downregulates Notch1, Hes1, AKT, mTORC1, S6K1, S6K2 and IL-17A mRNA expression, but upregulates PTEN mRNA expression. The mRNA expression levels of Notch1, Hes1, PTEN, AKT, mTORC1, S6K1, S6K2

and IL-17A in skin samples among the three experimental groups presented remarkable differences (all $P<0.05$; Table III; Fig. 5). In addition, further comparisons between two groups showed that the mRNA expression levels of Notch1, Hes1, AKT, mTORC1, S6K1, S6K2 and IL-17A were significantly higher in model mice than in control mice (all $P<0.05$; Table III; Fig. 5), while LY294002 inhibition resulted in a significantly reduced mRNA expression of the aforementioned molecules in the intervention mice (all $P<0.05$; Table III; Fig. 5). PTEN mRNA expression in model mice was significantly lower compared with that in control mice, but was considerably reversed by LY294002 treatment in intervention mice (both $P<0.01$; Table III; Fig. 5).

LY294002 inhibition reduces the protein levels of Notch1, NICD1, Hes1, p-AKT (Ser473), p-AKT (Thr308), p-mTOR (Ser2448), S6K1 (p70S6K), S6K2 (p70S6Kβ) and IL-17A, but increases PTEN protein levels. There were marked differences in the protein levels of Notch1, NICD1, Hes1, PTEN,

Table II. Inguinal lymph node weight, spleen mass and spleen index of experimental mice (each n=8).

Group	Inguinal lymph node weight (g)	Spleen mass (g)	Spleen index (mg/g)
Control	4.863±0.544	0.253±0.024	0.118±0.010
Model	15.760±0.716[a]	0.408±0.024[a]	0.214±0.013[a]
Intervention	9.943±0.701[b]	0.348±0.009[b]	0.175±0.006[b]

Data are presented as the means ± SD. One-way ANOVA followed by Student-Newman-Keuls test were used for statistical analysis. [a]$P<0.01$ vs. Control; [b]$P<0.01$ vs. Model.
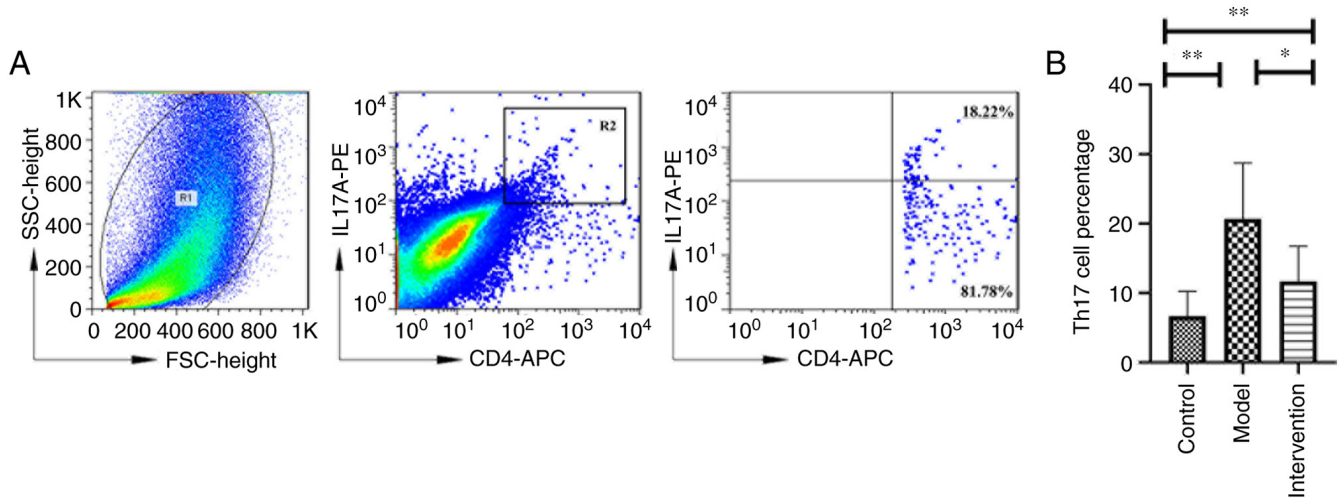

Figure 4. (A) Representative images of Th17 cell percentage in skin samples of experimental mice. (B) Comparison of Th17 cell percentage among the experimental mice. Data are presented as the means ± SD of the percentage of IL-17A^{+} CD4^{+} T cells/CD4^{+} T cells (control mice, 6.670±3.545%; model mice, 20.521±8.023%; and intervention mice, 11.540±5.278%) *$P<0.05$ and **$P<0.01$. Th, T helper.

p-AKT (Ser473), p-AKT (Thr308), p-mTOR (Ser2448), S6K1 (p70S6K), S6K2 (p70S6Kβ) and IL-17A in skin tissues among the three experimental groups (all $P<0.05$; Table IV; Fig. 6). The protein levels of Notch1, NICD1, Hes1, p-AKT (Ser473), p-AKT (Thr308), p-mTOR (Ser2448), S6K1 (p70S6K), S6K2 (p70S6Kβ) and IL-17A were higher in the model mice than in control mice (all $P<0.05$; Table IV; Fig. 6). However, upon LY294002 treatment, the expression of all of these proteins were markedly decreased in the intervention mice (all $P<0.05$). By contrast, the PTEN protein level was significantly reduced in model mice compared with that in control mice ($P<0.01$), whereas following LY294002 treatment, it was elevated in the intervention mice ($P<0.01$; Table IV; Fig. 6).

High dose of LY294002 presents even more obviously regulatory effect on the percentage of Th17 cells as well as mRNA expression and protein levels of Hes1, PTEN, AKT, mTORC1 and IL-17A. The percentage of Th17 cells, mRNA expression of Hes1, AKT, mTORC1 and IL-17A as well as protein levels of Hes1, p-AKT (Ser473), p-AKT (Thr308), p-mTOR (Ser2448) and IL-17A were significantly increased, while the expression levels of PTEN were obviously decreased in splenic mononuclear cells from 5% IMQ-induced mice compared with control mice ($P<0.01$; Tables V and VI; Figs. 7-9). LY294002 treatment on 5% IMQ-induced mouse splenic mononuclear cells dramatically reduced Th17 cell percentage, Hes1, AKT,

mTORC1 and IL-17A mRNA expression and their corresponding protein levels, while increased PTEN expression levels were confirmed in 50 μM LY294002-treated group ($P<0.01$; Tables V and VI; Figs. 7-9).

Discussion

Psoriasis is an immune-driven inflammatory disease, in which dendritic cells, T cells and keratinocytes serve critical roles (30). Originally, Th1 cells were considered to be the major mediators of psoriasis. Increasing evidence derived from animal and human studies suggested that Th17 cells and IL-17 may be major mediators of psoriasis (31,32). IL-17A is an important member of the IL-17 family (IL-17A-F). IL-17A is generally referred to as IL-17. IL-17 blockade, either via cytokine IL-17A or its receptor IL-17RA, can markedly reverse the clinical disease severity and molecular features of patients with psoriasis (4,33). Our previous research demonstrated increased IL-17A serum levels in patients with psoriasis, as well as elevated IL-17A levels both in the sera and skin tissues of mice with psoriasis-like skin inflammation (34-36). In the present study, elevated IL-17A mRNA and protein levels, as well as increased Th17 cell percentage were observed in mouse psoriasis-like skin lesions. Psoriasis is a systemic disease, associated with increased risk for comorbidities (37). It has been reported that IMQ can induce spleen enlargement

Table III. mRNA expression of Notch1, Hes1, PTEN, AKT, mTORC1, S6K1, S6K2 and IL-17A in skin samples of experimental mice (each n=8).

Group	Notch1	Hes1	PTEN	AKT	mTORC1	S6K1	S6K2	IL-17A
Control	0.966±0.442	0.617±0.501	1.369±0.411	1.024±0.238	1.021±0.224	0.789±0.189	0.621±0.305	0.302±0.156
Model	2.351±0.958[a]	3.704±1.823[a]	0.504±0.215[a]	3.864±0.891[a]	1.455±0.389[a]	1.323±0.313[a]	1.888±0.615[a]	1.097±0.543[a]
Intervention	1.178±0.590[b]	1.341±1.085[b]	1.052±0.359[b]	2.352±0.706[b]	1.030±0.274[c]	1.016±0.185[c]	1.015±0.189[b]	0.545±0.252[b]
F-value	9.146	13.154	13.361	35.941	5.339	11.473	19.893	10.402
P-value	<0.01	<0.01	<0.01	<0.01	<0.05	<0.01	<0.01	<0.01

Data are presented as the means ± SD. One-way ANOVA followed by Student-Newman-Keuls test are used for statistical analysis. [a]$P<0.01$ vs. Control; [b]$P<0.01$ and [c]$P<0.05$ vs. Model. Hes1, Hairy/enhancer of split 1; PTEN, Phosphatase and tensin homolog deleted on chromosome ten; mTORC1, mammalian target of rapamycin complex 1; S6K1, S6 kinase 1; S6K2, S6 kinase 2; IL-17A, interleukin-17A.
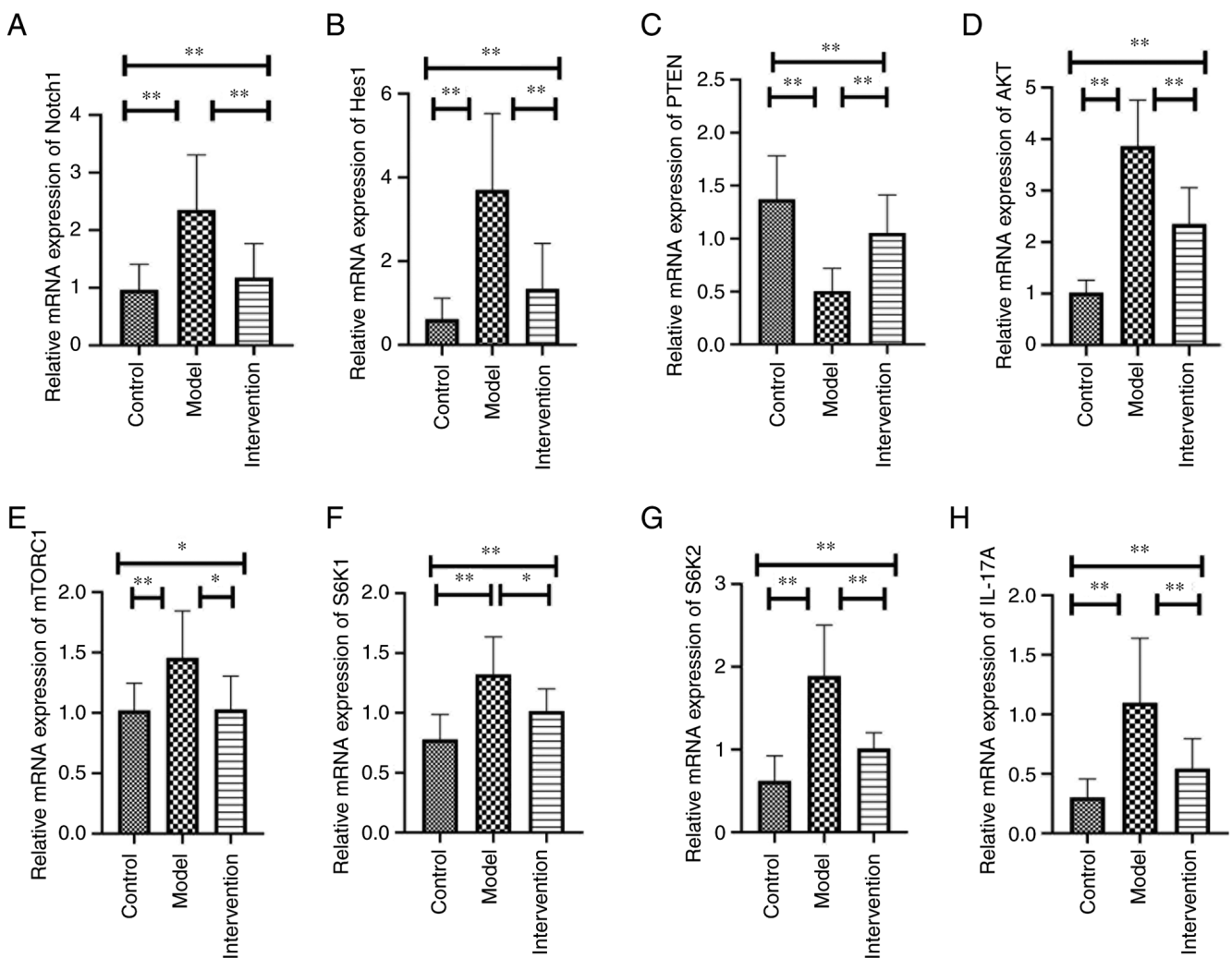

Figure 5. mRNA expression of (A) Notch1, (B) hairy and enhancer of split 1, (C) PTEN, (D) AKT, (E) mTOR complex 1, (F) S6K1, (G) S6K2 and (H) IL-17A in skin samples of experimental mice. $^*P<0.05$ and $^{**}P<0.01$. S6K, S6 kinase.

through systemic effects and alter the immune cell composition of IMQ-induced psoriatic model mice (38,39). Our previous study also demonstrated an increased percentage in Th17 cells in splenic CD4$^+$ T cells in this type of psoriatic mouse model (33). Additionally, the present study detected enlarged spleen and inguinal lymph nodes, further indicating its enhanced systemic inflammatory response in mouse psoriasis-like inflammation. Upon effective interruption by LY294002, splenomegaly and lymphadenopathy were fully mitigated (Table II; Fig. 3).

Th17 cell differentiation is regulated by a complex network of transcription factors and intracellular signaling

Table IV. Protein levels of Notch1, NICD1, Hes1, PTEN, p-AKT (Thr308), p-AKT (Ser473), p-mTOR (Ser2448), S6K1 (p70s6kα), S6K2 (p70s6kβ) and IL-17A in skin samples of experimental mice (each n=8).

Group	Notch1	NICD1	Hes1	PTEN	p-AKT(Thr308)
Control	0.688±0.365	0.996±0.205	0.735 (0.130)	1.011±0.077	0.908±0.273
Model	1.211±0.339[b]	1.229±0.095[b]	1.188 (0.680)[b]	0.770±0.053[a]	1.928±0.536[a]
Intervention	0.824±0.220[d]	0.798±0.141[c]	0.819 (0.210)[d]	0.984±0.079[c]	1.111±0.540[d]
F-value/χ^2	4.476	11.800	9.696	21.027	8.037
P-value	<0.05	<0.01	<0.01	<0.01	<0.01

Group	p-AKT (Ser473)	p-mTOR (Ser2448)	S6K1	S6K2	IL-17A
Control	0.601±0.190	0.843 (0.190)	0.731±0.205	0.824 (0.63)	0.905±0.084
Model	1.226±0.696[b]	1.184 (0.900)[b]	0.936±0.128[b]	1.419 (0.990)[a]	1.396±0.250[a]
Intervention	0.659±0.197[d]	0.920 (0.200)[d]	0.667±0.073[c]	0.839 (0.440)[d]	1.033±0.159[c]
F-value/χ^2	3.833	8.983	5.577	10.433	12.310
P-value	<0.05	<0.05	<0.05	<0.01	<0.01

Data are presented as the means ± SD and median (interquartile range). One-way ANOVA followed by Student-Newman-Keuls test and Kruskal-Wallis H test followed by the Dunn-Bonferroni test are used for statistical analysis. [a]P<0.01 and [b]P<0.05 vs. Control; [c]P<0.01 and [d]P<0.05 vs. Model. NICD, Notch intracellular domain; Hes1, Hairy/enhancer of split 1; PTEN, Phosphatase and tensin homolog deleted on chromosome ten; mTOR, mammalian target of rapamycin; S6K1, S6 kinase 1; S6K2, S6 kinase 2; IL-17A, interleukin-17A; p-, phosphorylated.

Table V. mRNA expression of Hes1, PTEN, AKT, mTORC1 and IL-17A and Th17 cell percentage in splenic mononuclear cells of experimental mice (each n=6).

Group	Hes1	PTEN	AKT	mTORC1	IL-17A	Th17 cell percent (%)
0 μM LY294002	0.914±0.135	0.444±0.087	0.939±0.107	0.959±0.105	1.005±0.406	9.074±2.381
10 μM LY294002	0.698±0.144	0.654±0.160[b]	0.720±0.156	0.764±0.095	0.682±0.260	7.130±1.449
50 μM LY294002	0.497±0.163[a]	0.806±0.157[a]	0.522±0.200[a]	0.546±0.175[a]	0.334±0.149[a]	5.024±1.410[a]
Control	0.281±0.125[a,c]	1.031±0.055[a,c]	0.329±0.110[a,c]	0.293±0.207[a,c]	0.175±0.054[a,d]	2.305±0.469[a,c]
F-value	21.728	24.183	18.815	21.005	12.772	20.261
P-value	<0.01	<0.01	<0.01	<0.01	<0.01	<0.01

Data are presented as the means ± SD. One-way ANOVA followed by Tukey's post hoc test were used for statistical analysis. [a]P<0.01 and [b]P<0.05 vs. 0 μM LY294002 group; [c]P<0.01 and [d]P<0.05 vs. 10 μM LY294002 group. Hes1, Hairy/enhancer of split 1; PTEN, Phosphatase and tensin homolog deleted on chromosome ten; mTORC1, mammalian target of rapamycin complex 1; IL-17A, interleukin-17A.

cascades, including PI3K/AKT/mTOR complexes, which are tightly regulated by feedback loops, in part through mTOR linkage with AKT (40). Two major pathways have been reported to intersect at AKT, namely the PI3K/p-AKT (Thr308)/mTORC1 and mTORC2/p-AKT (Ser473)/FOXO1/3a signaling pathways (41). The roles of secondary messengers in Th17 differentiation remain contested, although several distinct signaling pathways have been confirmed to regulate Th17 differentiation through mTORC1 (20). S6K is an important downstream target of mTORC1, and presents high homology with the kinases S6K1 and S6K2. PI3K/AKT/mTORC1/S6K1/2 signaling has been reported to control Th17 cell differentiation by regulating RORγt nuclear translocation and the expression of the Th17 cell differentiation negative regulator Gfi1 (19). The present study demonstrated a significant increase in Th17 cell percentage,

as well as in the mRNA and protein expression levels of AKT, mTORC1, S6K1, S6K2 and IL-17A in skin lesions of psoriatic model mice (Figs. 4-6), which confirmed that PI3K/AKT signaling was involved in the pathogenesis of psoriasis. To further evaluate the possible effect of PI3K/AKT on Th17 cell differentiation and IL-17A production in the disease-specific inflammation process of psoriasis, PI3K/AKT signaling was blocked by LY294002, which resulted in a coordinated decrease in the aforementioned increased levels of PI3K/AKT signaling molecules AKT, mTORC1, S6K1 and S6K2 as well as Th17 cell percentage with its effector cytokine IL-17A in intervention mice (Figs. 4-6). Importantly, marked alleviation of psoriasiform inflammation, thickened epidermis and inflammatory cell-infiltrated dermis were also observed in intervention mice (Figs. 1 and 2). Therefore, our previous study together with the current findings suggested that the
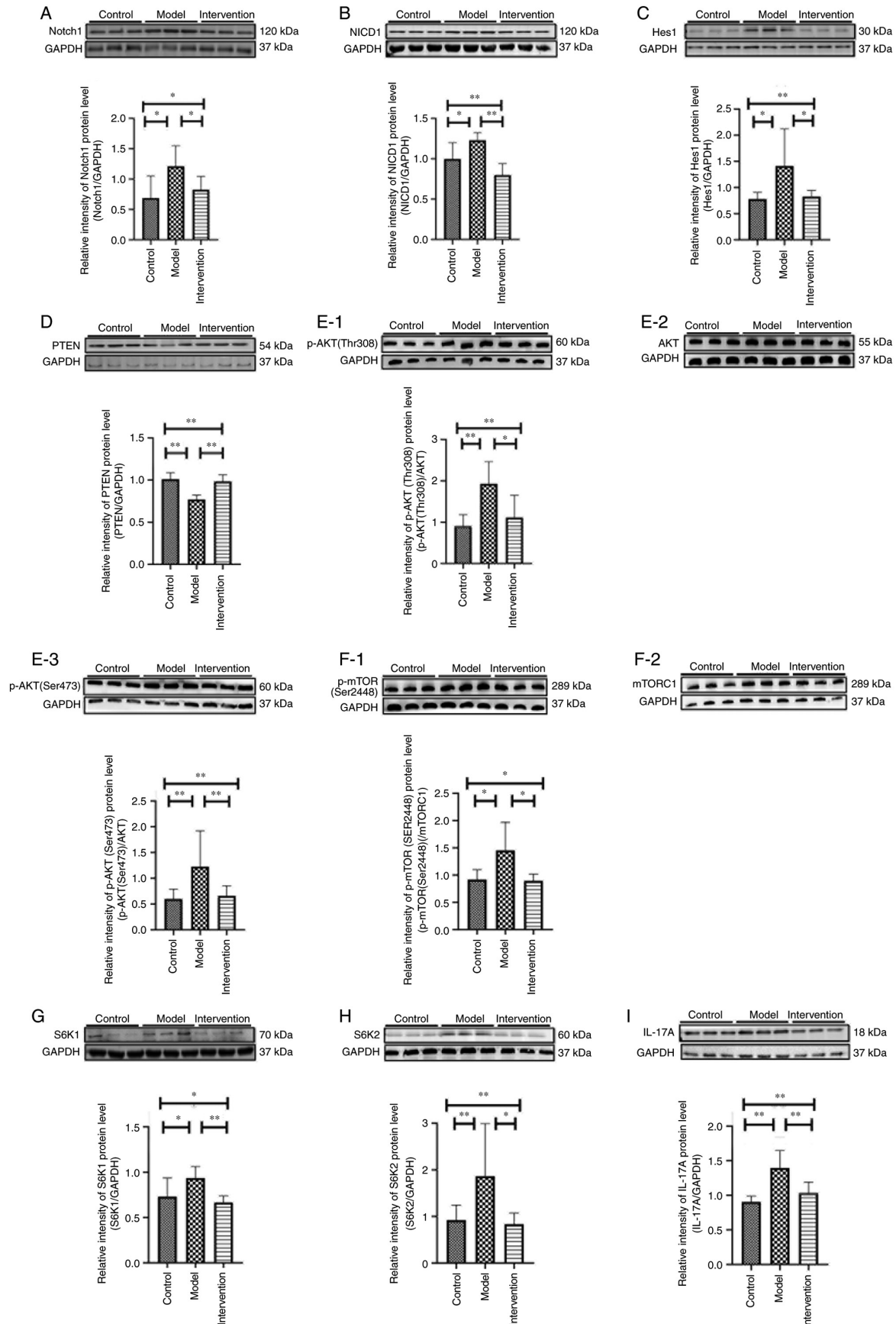
Figure 6. Protein levels of (A) Notch1, (B) NICD1, (C) hairy and enhancer of split 1, (D) PTEN, (E-1) p-AKT (Thr308), (E-2) AKT, (E-3) p-AKT (Ser473), (F-1) p-mTOR (Ser2448), (F-2) mTORC1, (G) S6K1 (p70S6Kα), (H) S6K2 (p70S6Kβ) and (I) IL-17A in skin samples of experimental mice. *P<0.05 and **P<0.01. NICD1, Notch intracellular domain 1; p, phosphorylated; S6K, S6 kinase. Since protein bands of p-AKT (Thr308), p-AKT (Ser473) and AKT are not from the same western blot membrane, they are evaluated with each corresponding loading control, then the protein levels of p-AKT (Thr308) and p-AKT (Ser473) are calculated by comparing with that of AKT. Similarly, protein bands of p-mTOR (Ser2448) and mTORC1 are evaluated with each corresponding loading control, then the protein level of p-mTOR (Ser2448) is calculated by comparing with that of mTORC1.

Table VI. Protein levels of Hes1, PTEN, p-AKT(Thr308), p-AKT(Ser473), p-mTOR (Ser2448) and IL-17A in splenic mono-nuclear cells of experimental mice (each n=6).

Group	Hes1	PTEN	p-AKT (Thr308)	p-AKT (Ser473)	p-mTOR (Ser2448)	IL-17A
0 μM LY294002	1.179±0.060	0.530±0.149	1.264±0.072	1.304±0.065	1.256±0.095	1.173±0.134
10 μM LY294002	0.939±0.070[a]	0.788±0.097[a]	0.992±0.077[a]	1.039±0.088[a]	1.026±0.061[a]	0.951±0.074[a]
50 μM LY294002	0.756±0.073[a,b]	0.948±0.100[a]	0.845±0.062[a,c]	0.866±0.108[a,c]	0.857±0.109[a,c]	0.810±0.085[a]
Control	0.569±0.111[a,b]	1.151±0.119[a,b]	0.608±0.073[a,b]	0.450±0.084[a,b]	0.550±0.107[a,b]	0.522±0.107[a,b]
F-value	62.235	29.712	88.796	100.548	58.847	42.321
P-value	<0.01	<0.01	<0.01	<0.01	<0.01	<0.01

Data are presented as the means ± SD. One-way ANOVA followed by Tukey's test are used for statistical analysis. [a]P<0.01 vs. 0 μM LY294002; [b]P<0.01, [c]P<0.05 vs. 10 μM LY294002. Hes1, Hairy/enhancer of split 1; PTEN, Phosphatase and tensin homolog deleted on chromosome ten; mTOR, mammalian target of rapamycin; IL-17A, interleukin-17A.
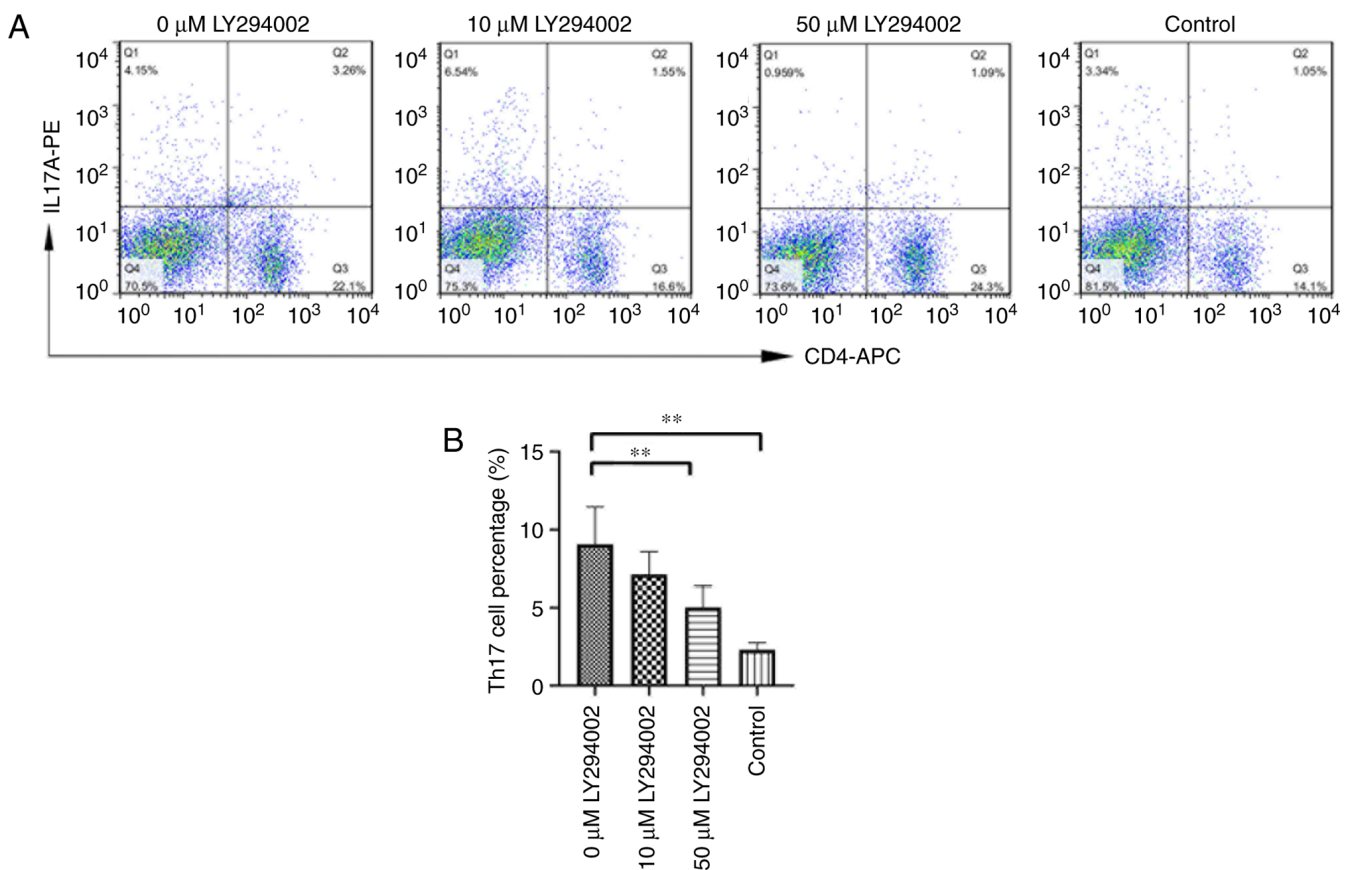

Figure 7. (A) Representative images of Th17 cell percentage in mouse splenic mononuclear cells of control group, 0 μM LY294002 group, 10 μM LY294002 group and 50 μM LY294002 group. (B) Comparison of the Th17 cell percentage in the four experimental groups. Data are presented as the mean ± SD of the percentage of IL-17A⁺ CD4⁺ T cells/CD4⁺ T cells (0 μM LY294002 group, 9.074±2.381%; 10 μM LY294002 group, 7.130±1.449%; 50 μM LY294002 group, 5.024±1.410%; control group, 2.305±0.469%) **P<0.01. Th, T helper.

PI3K/AKT/mTORC1/S6K1/2 axis can exert its function in the development of psoriasis by regulating Th17 cells.

Notch signaling plays a critical role in the lineage commitment of cells and fates of lymphocytes, and is also well known for its pivotal role in Th17 cell differentiation (10,11,41). Notch signaling is initiated through the binding of the Notch receptor with a Notch ligand; subsequently, a series of enzymatic reactions result in the cleavage of NICD by γ-secretase. NICD is then translocated to the nucleus, where it activates the transcription of downstream genes (42). Thus, Notch signaling activation is controlled by γ-secretase. The effects of γ-secretase inhibitors on murine and human Th17 cell differentiation have been reported, leading to a marked reduction in IL-17A production (11). Our previous research verified increased expression of Notch1 and its target gene Hes1 in patients with psoriasis and in a mouse model of psoriasis, and demonstrated that the γ-secretase inhibitor DAPT could notably decrease IL-17A production
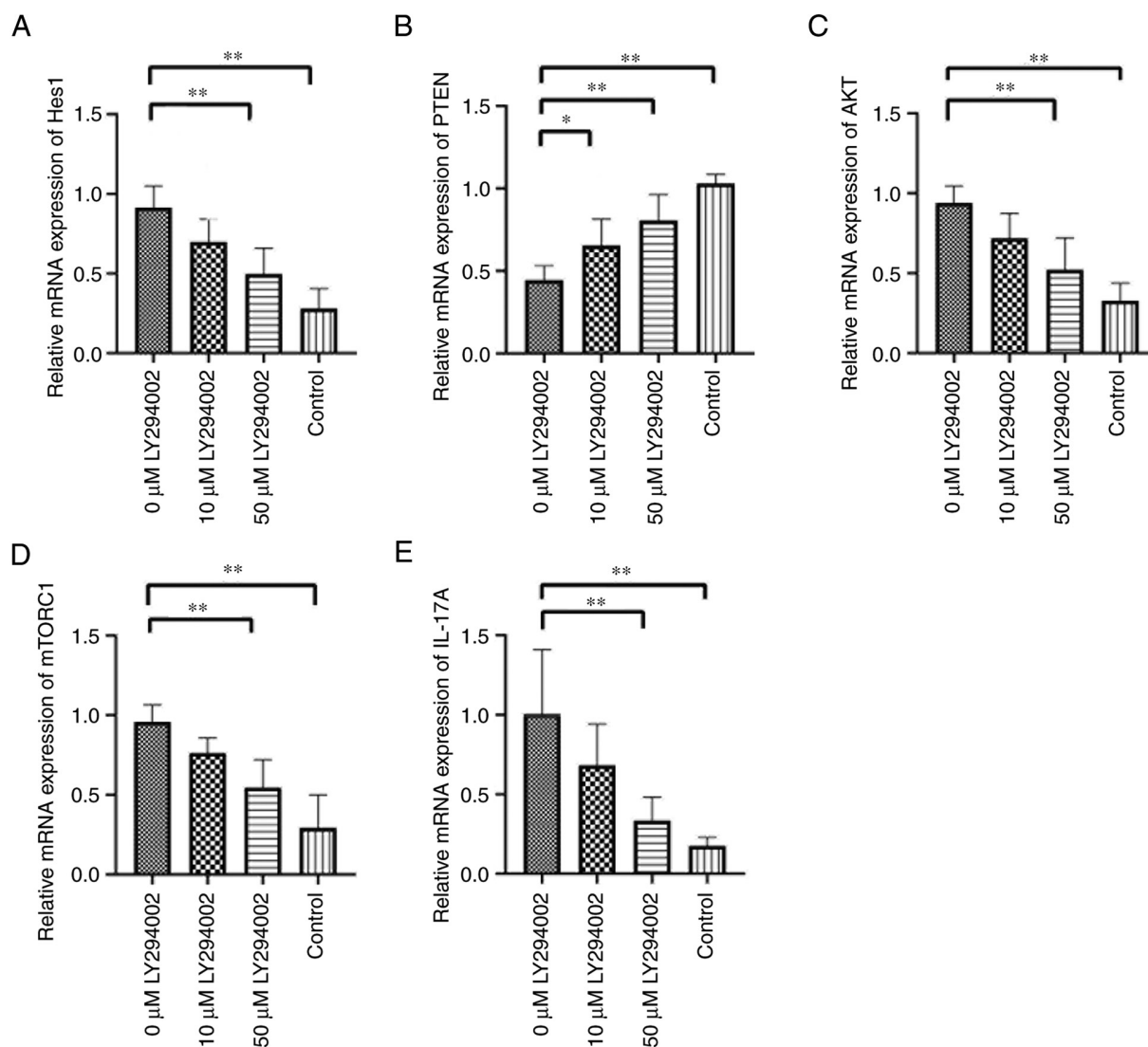
Figure 8. mRNA expression of (A) hairy and enhancer of split 1, (B) PTEN, (C) AKT, (D) mTOR complex 1 and (E) IL-17A in mouse splenic mononuclear cells of control group, 0 μM LY294002 group, 10 μM LY294002 group and 50 μM LY294002 group. *P<0.05 and **P<0.01.

by CD4^{+} T cells in Th17 polarizing situations, both in psoriasiform mice and in patients with psoriasis (13,35). Signal transduction is a complex network involving numerous intercellular signaling molecules, interactions, crosstalk and feedback loops. PTEN is a crucial negative regulator of PI3K/AKT/mTOR signaling, which was demonstrated to be markedly decreased in psoriasiform skin of model mice in the present study (Figs. 5 and 6). Notch1 plays an important role in regulating the expression of PTEN and the activity of PI3K/AKT signaling through Hes1 (21,43,44). The Notch1/Hes1/PTEN signaling axis has been reported to be involved in certain human diseases (21-27). In hepatocellular carcinoma cells, knockdown of Notch1 was correlated with the reduction of p-AKT (26). Downregulation of Notch1 resulted in PTEN activation and AKT dephosphorylation, and inhibited the invasion and metastasis of the human gastric cancer cell lines SGC7901 and MKN74 (27). In addition, promoter dual luciferase reporter assays demonstrated that the PTEN DNA sequence has promoter activity. Hes1 binds to the PTEN promoter region and can directly regulate the

promoter of PTEN, leading to the activation of PI3K/AKT signaling (24). Thus, the Hes1-mediated negative regulation of PTEN to activate the PI3K/AKT/mTORC1/S6K1/2 axis may be an important mechanism of Notch1/Hes1 signaling driving Th17 cell differentiation and IL-17A production.

In addition, Notch1 activation induced by IL-17 has been confirmed to occur via the signaling molecule Act1, which is a critical adaptor molecule in IL-17 signaling transduction (14,15). The crosstalk of IL-17 with Notch1 was first demonstrated in oligodendrocyte progenitor cells (14). IL-17R interacts with Notch1 through its extracellular domain, thus forming the Act1-NICD1 complex and subsequently translocating into nuclei (14). As a result, Act1 and the transcription factor recombination signal binding protein for immunoglobulin kJ region, the core element of Notch signaling, are recruited to the promoters of Th17-induced Notch1 target genes (15). Based on the aforementioned studies, it can be proposed that a feedback loop of Notch1/Hes1-PTEN/PI3K/AKT/mTORC1/S6K1/2 may exist to mediate the effects of IL-17A. The present study
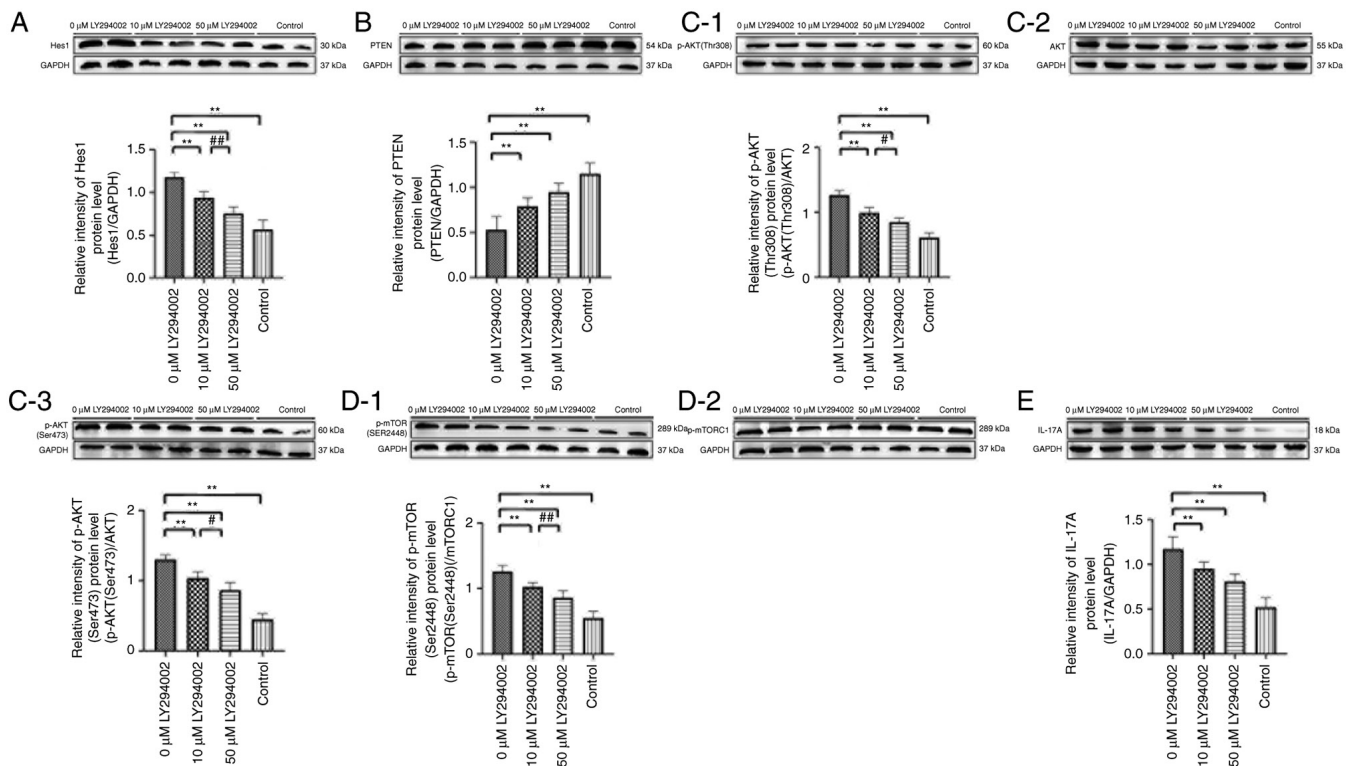
Figure 9. Protein levels of (A) hairy and enhancer of split 1, (B) PTEN, (C-1) p-AKT (Thr308), (C-2) AKT, (C-3) p-AKT (Ser473), (D-1) mTORC1, (D-2) p-mTOR (Ser2448), (E) IL-17A in mouse splenic mononuclear cells of control group, 0 μM LY294002 group, 10 μM LY294002 group and 50 μM LY294002 group. **$P<0.01$, #$P<0.05$ and ##$P<0.01$. p-, phosphorylated. Since protein bands of p-AKT (Thr308), p-AKT (Ser473) and AKT are not from the same western blot membrane, they are evaluated with each corresponding loading control, then the protein levels of p-AKT (Thr308) and p-AKT (Ser473) are calculated by comparing with that of AKT. Similarly, protein bands of p-mTOR (Ser2448) and mTORC1 are evaluated with each corresponding loading control, then the protein level of p-mTOR (Ser2448) is calculated by comparing with that of mTORC1.

confirmed increased mRNA and protein expression levels of Notch1, NICD1 and Hes1; decreased PTEN; elevated p-AKT, p-mTORC1, S6K1 and S6K2; and increased Th17 cell percentage and IL-17A levels in mouse psoriasis-like skin inflammation, which further demonstrated that both the PI3K/AKT and Notch1 signaling pathways are hyperactivated in psoriasis and play important roles in the pathogenesis of psoriasis. To corroborate the crosstalk and feedback loop of Notch1/Hes1-PTEN/PI3K/AKT/mTORC1/S6K1/2 around Th17 cells and IL-17A, PI3K/AKT signaling was inhibited by LY294002 while establishing a model of psoriasiform inflammation. Following LY294002 inhibition, with the exception of reduced expression of AKT, mTORC1, S6K1, S6K2 and IL-17A as well as Th17 cell percentage, decreased Notch1, NICD1 and Hes1 were observed as well as increased PTEN, which suggested the action of IL-17A crosstalk with Notch1 and the continuous feedback loop of Notch1/Hes1-PTEN/PI3K/AKT/mTORC1/S6K1/2 around IL-17A. Our study group have focused on the studies of Th17 cells and IL-17A for more than ten years, especially in the field of atopic dermatitis and psoriasis (13,34-36,45,46). In recent five years, close attention was paid to the regulatory effect of Notch1/Hes1 signaling on Th17 cell and γδT17 cell differentiation in psoriasis, and related *in vitro/in vivo* studies were performed through blocking Notch1/Hes1 signaling by γ-secretase inhibitor and it was reported that Notch1 inhibition by DAPT could significantly suppress Th17 cell differentiation and IL-17A production (13,35,36). In the present study,

for the first time, Notch1/Hes1-PTEN/AKT/IL-17A feedback loop was proposed, the crosstalk between Notch1/Hes1 signaling and PI3K/AKT/mTORC1 signaling and their coordinate regulatory effect on Th17 cell differentiation in psoriatic inflammation. A study on metastasis of gastric cancer revealed that the PI3K/AKT and Notch1 signaling blockers LY294002 and DAPT coordinately inhibited the metastasis of gastric cancer through mutual enhancement (47). Thus, based on our previous findings and the present results, the Notch1/Hes1-PTEN/AKT/IL-17A feedback loop may be an important mechanism in the regulation of Th17 differentiation in psoriasis. Blocking the Notch1/Hes1-PTEN/AKT/IL-17A feedback loop may be a potential therapeutic method for the treatment of psoriatic inflammation.

IMQ-induced mouse psoriasis-like skin inflammation reached peak severity at day 7-8, then diminished gradually (48), thus in most of mouse psoriatic inflammation studies established by 5% IMQ, mice were administered a daily topical application for 6-7 consecutive days. Due to the short duration of classic psoriatic features and character of gradual diminishment, LY294002 intervention was conducted at the same time of experimental model establishment. The limitation of the present study is that it did not explore the intervention effects of different dose of LY294002 on experimental mice and their intervention effects after the establishment of psoriatic lesions. In the *in vitro* experiment of the present study, 10 and 50 μM LY294002 were exerted on splenic mononuclear cells from 5% IMQ-induced mice;

notably, the even more obvious intervention effects of 50 μM LY294002 were confirmed. Related *in vitro/in vivo* studies shall be performed in the future to more deeply evaluate the potential therapeutic effect of LY294002 in psoriatic inflammation.

Availability of data and materials

All data generated or analyzed during this study are included in this manuscript or are available from the corresponding author on reasonable request.

Authors' contributions

YWL and XXL carried out the experiments, performed the statistical analysis and wrote the first draft of the manuscript. FHF participated in the design of the study and carried out the experiments, particularly for the development of the experimental model. BL and RQQ participated in the design of the study and analyzed the data. XYX helped to carry out the experiments. LM was responsible for the design of the study, reviewed and edited this article. All authors read and approved the final manuscript and agree to be accountable for all aspects of the work in ensuring that questions related to the accuracy or integrity of the work are appropriately investigated and resolved. LM and YWL confirm the authenticity of all the raw data.

Ethics approval and consent to participate

The present study was approved (approval no. 20190104-15) by the Laboratory Animal Ethics Committee of Binzhou Medical University Hospital (Binzhou, China).

Patient consent for publication

Not applicable.

Competing interests

The authors declare that they have no competing interests.

References

1. Yamanaka K, Yamamoto O and Honda T: Pathophysiology of psoriasis: A review. J Dermatol 48: 722-731, 2021.
2. Furue K, Ito T, Tsuji G, Kadono T and Furue M: Psoriasis and the TNF/IL23/IL17 axis. G Ital Dermatol Venereol 154: 418-424, 2019.
3. Molinelli E, Campanati A, Brisigotti V and Offidani A: Biologic therapy in psoriasis (part II): Efficacy and safety of new treatment targeting IL23/IL-17 pathways. Curr Pharm Biotechnol 18: 964-978, 2017.
4. Ly K, Smith MP, Thibodeaux Q, Reddy V, Liao W and Bhutani T: Anti IL-17 in psoriasis. Expert Rev Clin Immunol 15: 1185-1194, 2019.
5. van der Fits L, Mourits S, Voerman JS, Kant M, Boon L, Laman JD, Cornelissen F, Mus AM, Florencia E, Prens EP and Lubberts E: Imiquimod-induced psoriasis-like skin inflammation in mice is mediated via the IL-23/IL-17 axis. J Immunol 182: 5836-5845, 2009.
6. Gratton R, Tricarico PM, Moltrasio C, Lima Estevão de Oliveira AS, Brandão L, Marzano AV, Zupin L and Crovella S: Pleiotropic role of Notch signaling in human skin diseases. Int J Mol Sci 21: 4214, 2020.
7. Gratton R, Tricarico PM, d'Adamo AP, Bianco AM, Moura R, Agrelli A, Brandão L, Zupin L and Crovella S: Notch signaling regulation in autoinflammatory diseases. Int J Mol Sci 21: 8847, 2020.
8. Fiúza UM and Arias AM: Cell and molecular biology of Notch. J Endocrinol 194: 459-474, 2007.
9. Auderset F, Coutaz M and Tacchini-Cottier F: The role of Notch in the differentiation of CD4$^+$ T helper cells. Curr Top Microbiol Immunol 360: 115-134, 2012.
10. Eagar TN, Tang Q, Wolfe M, He Y, Pear WS and Bluestone JA: Notch 1 signaling regulates peripheral T cell activation. Immunity 20: 407-415, 2004.
11. Keerthivasan S, Suleiman R, Lawlor R, Roderick J, Bates T, Minter L, Anguita J, Juncadella I, Nickoloff BJ, Le Poole IC, *et al*: Notch signaling regulates mouse and human Th17 differentiation. J Immunol 187: 692-701, 2011.
12. Radtke F, Fasnacht N and MacDonald HR: Notch signaling in the immune system. Immunity 32: 14-27, 2010.
13. Ma L, Xue H, Qi R, Wang Y and Yuan L: Effect of γ-secretase inhibitor on Th17 cell differentiation and function of mouse psoriasis-like skin inflammation. J Transl Med 16: 59, 2018.
14. Qian Y, Liu C, Hartupee J, Altuntas CZ, Gulen MF, Jane-Wit D, Xiao J, Lu Y, Giltiay N, Liu J, *et al*: The adaptor Act1 is required for interleukin 17-dependent signaling associated with autoimmune and inflammatory disease. Nat Immunol 8: 247-256, 2007.
15. Wang C, Zhang CJ, Martin BN, Bulek K, Kang Z, Zhao J, Bian G, Carman JA, Gao J, Dongre A, *et al*: IL-17 induced NOTCH1 activation in oligodendrocyte progenitor cells enhances proliferation and inflammatory gene expression. Nat Commun 8: 15508, 2017.
16. Weichhart T and Säemann MD: The PI3K/Akt/mTOR pathway in innate immune signaling: Emerging therapeutic applications. Ann Rheum Dis 67 (Suppl 3): iii70-iii74, 2008.
17. Mercurio L, Albanesi C and Madonna S: Recent updates on the involvement of PI3K/AKT/mTOR molecular cascade in the pathogenesis of hyperproliferative skin disorders. Front Med (Lausanne) 8: 665647, 2021.
18. Chamcheu JC, Chaves-Rodriquez MI, Adhami VM, Siddiqui IA, Wood GS, Longley BJ and Mukhtar H: Upregulation of PI3K/AKT/mTOR, FABP5 and PPARβ/δ in human psoriasis and imiquimod-induced murine psoriasiform dermatitis model. Acta Derm Venereol 96: 854-856, 2016.
19. Kurebayashi Y, Nagai S, Ikejiri A, Ohtani M, Ichiyama K, Baba Y, Yamada T, Egami S, Hoshii T, Hirao A, *et al*: PI3K-Akt-mTORC1-S6K1/2 axis controls Th17 differentiation by regulating Gfi1 expression and nuclear translocation of RORγ. Cell Rep 1: 360-373, 2012.
20. Nagai S, Kurebayashi Y and Koyasu S: Role of PI3K/Akt and mTOR complexes in Th17 cell differentiation. Ann N Y Acad Sci 1280: 30-34, 2013.
21. Palomero T, Sulis ML, Cortina M, Real PJ, Barnes K, Ciofani M, Caparros E, Buteau J, Brown K, Perkins SL, *et al*: Mutational loss of PTEN induces resistance to NOTCH1 inhibition in T-cell leukemia. Nat Med 13: 1203-1210, 2007.
22. Hales EC, Taub JW and Matherly LH: New insights into Notch1 regulation of the PI3K-AKT-mTOR1 signaling axis: Targeted therapy of γ-secretase inhibitor resistant T-cell acute lymphoblastic leukemia. Cell Signal 26: 149-161, 2014.
23. Li X, Zou F, Lu Y, Fan X, Wu Y, Feng X, Sun X and Liu Y: Notch1 contributes to TNF-α-induced proliferation and migration of airway smooth muscle cells through regulation of the Hes1/PTEN axis. Int Immunopharmacol 88: 106911, 2020.
24. Liu X, Zhang Y, Shi M, Wang Y, Zhang F, Yan R, Liu L, Xiao Y and Guo B: Notch1 regulates PTEN expression to exacerbate renal tubulointerstitial fibrosis in diabetic nephropathy by inhibiting autophagy via interactions with Hes1. Biochem Biophys Res Commun 497: 1110-1116, 2018.
25. Tian T, Fu X, Lu J, Ruan Z, Nan K, Yao Y and Yang Y: MicroRNA-760 inhibits doxorubicin resistance in hepatocellular carcinoma through regulating Notch1/Hes1-PTEN/Akt signaling pathway. J Biochem Mol Toxicol 32: e22167, 2018.

26. Zhang X, Hu Y, Gao H, Lan X and Xue Y: Downregulation of Notch1 inhibits the invasion and metastasis of human gastric cancer cells SGC7901 and MKN74 *in vitro* through PTEN activation and dephosphorylation of AKT and FAK. Mol Med Rep 16: 2318-2324, 2017.

27. Sokolowski KM, Balamurugan M, Kunnimalaiyaan S, Wilson J, Gamblin TC and Kunnimalaiyaan M: Role of Akt inhibition on Notch1 expression in hepatocellular carcinoma: Potential role for dual targeted therapy. Am J Surg 211: 755-760, 2016.

28. Lan XO, Wang HX, Qi RQ, Xu YY, Yu YJ, Yang Y, Guo H, Gao XH and Geng L: Shikonin inhibits CEBPD downregulation in IL-17-treated HaCaT cells and in an imiquimod-induced psoriasis model. Mol Med Rep 22: 2263-2272, 2020.

29. Livak KJ and Schmittgen TD: Analysis of relative gene expression data using real-time quantitative PCR and the 2(-Delta Delta C(T)) method. Methods 25: 402-408, 2001.

30. Greb JE, Goldminz AM, Elder JT, Lebwohl MG, Gladman DD, Wu JJ, Mehta NN, Finlay AY and Gottlieb AB: Psoriasis. Nat Rev Dis Primers 2: 16082, 2016.

31. Di Cesare A, Di Meglio P and Nestle FO: The IL-23/Th17 axis in the immunopathogenesis of psoriasis. J Invest Dermatol 129: 1339-1350, 2009.

32. Li B, Huang L, Lv P, Li X, Liu G, Chen Y, Wang Z, Qian X, Shen Y, Li Y and Fang W: The role of Th17 cells in psoriasis. Immunol Res 68: 296-309, 2020.

33. Hawkes JE, Chan TC and Krueger JG: Psoriasis pathogenesis and the development of novel targeted immune therapies. J Allergy Clin Immunol 140: 645-653, 2017.

34. Ma L, Xue HB, Guan XH, Shu CM, Wang F, Zhang JH and An RZ: The imbalance of Th17 cells and CD4(+) CD25(high) Foxp3(+) Treg cells in patients with atopic dermatitis. J Eur Acad Dermatol Venereol 28:1079-1086, 2014.

35. Ma L, Xue H, Gao T, Gao M and Zhang Y: Notch1 signaling regulates the Th17/Treg immune imbalance in patients with psoriasis vulgaris. Mediators Inflamm 2018: 3069521, 2018.

36. Wang Y, Li X, Xing X, Xue H, Qi R, Ji H and Ma L: Notch-Hes1 signaling regulates IL-17A^{+} γδ [+]T cell expression and IL-17A secretion of mouse psoriasis-like skin inflammation. Mediators Inflamm 2020: 8297134, 2020.

37. Korman NJ: Management of psoriasis as a systemic disease: What is the evidence? Br J Dermatol 182: 840-848, 2020.

38. Kim CH, Yoo JK, Jeon SH, Lim CY, Lee JH, Koo DB and Park MY: Anti-psoriatic effect of myeloid-derived suppressor cells on imiquimod-induced skin inflammation in mice. Scand J Immunol 89: e12742, 2019.

39. Frenzel DF, Borkner L, Scheurmann J, Singh K, Scharffetter-Kochanek K and Weiss JM: Osteopontin deficiency affects imiquimod-induced psoriasis-like murine skin inflammation and lymphocyte distribution in skin, draining lymph nodes and spleen. Exp Dermatol 24: 305-307, 2015.

40. Chamcheu JC, Adhami VM, Esnault S, Sechi M, Siddiqui IA, Satyshur KA, Syed DN, Dodwad SJ, Chaves-Rodriquez MI, Longley BJ, *et al*: Dual inhibition of PI3K/Akt and mTOR by the dietary antioxidant, delphinidin, ameliorates psoriatic features in vitro and in an imiquimod-induced psoriasis-like disease in mice. Antioxid Redox Signal 26: 49-69, 2017.

41. Coutaz M, Hurrell BP, Auderset F, Wang H, Siegert S, Eberl G, Ho PC, Radtke F and Tacchini-Cottier F: Notch regulates Th17 differentiation and controls trafficking of IL-17 and metabolic regulators within Th17 cells in a context-dependent manner. Sci Rep 6: 39117, 2016.

42. Nagase H and Nakayama K: γ-Secretase-regulated signaling typified by Notch signaling in the immune system. Curr Stem Cell Res Ther 8: 341-356, 2013.

43. Palomero T, Dominguez M and Ferrando AA: The role of the PTEN/AKT pathway in NOTCH1-induced leukemia. Cell Cycle 7: 965-970, 2008.

44. Liu S, Ma X, Ai Q, Huang Q, Shi T, Zhu M, Wang B and Zhang X: NOTCH1 functions as an oncogene by regulating the PTEN/PI3K/AKT pathway in clear cell renal cell carcinoma. Urol Oncol 31: 938-948, 2013.

45. Ma L, Xue HB, Guan XH, Qi RQ, An RZ, Shu CM, Zhang YJ, Wei YH and Zhang JH: Possible role of Th17 cells and IL-17 in the pathogenesis of atopic dermatitis in northern China. J Dermatol Sci 68: 66-68, 2012.

46. Ma L, Xue HB, Wang F, Shu CM and Zhang JH: MicroRNA-155 may be involved in the pathogenesis of atopic dermatitis by modulating the differentiation and function of T helper type 17 (Th17) cells. Clin Exp Immunol 181:142-149, 2015.

47. Peng X, Zhou J, Li B, Zhang T, Zuo Y and Gu X: Notch1 and PI3K/Akt signaling blockers DAPT and LY294002 coordinately inhibit metastasis of gastric cancer through mutual enhancement. Cancer Chemother Pharmacol 85: 309-320, 2020.

48. Zhao J, Di T, Wang Y, Liu X, Liang D, Zhang G and Li P: Multi-glycoside of tripterygium wilfordii Hook. f. ameliorates imiquimod-induced skin lesions through a STAT3-dependent mechanism involving the inhibition of Th17-mediated inflammatory responses. Int J Mol Med 38: 747-757, 2016.